Missouri University of Science and Technology

Scholars' Mine

International Specialty Conference on Cold-Formed Steel Structures

(1978) - 4th International Specialty Conference on Cold-Formed Steel Structures

Jun 1st, 12:00 AM

European Research on Pallet, Drive-in and Drive-through Racks

Jan W. B. Stark

Kees Tilburgs

Follow this and additional works at: https://scholarsmine.mst.edu/isccss

Part of the Structural Engineering Commons

Recommended Citation

EUROPEAN RESEARCH ON PALLET, DRIVE-IN and DRIVE-THROUGH RACKS

by Jan Stark[*] and Kees Tilburgs[**]

SUMMARY

This paper presents a review of research on storage racking. The research program is financially supported by the Dutch industry and the ECSC[***], and is carried out in cooperation with laboratories in four European countries. Results in this paper relate to pallet rack design in terms of completed parts of the Dutch contribution to this European program.

----

[*]   Head of the Department of Steel Structures, Institute TNO for Building Materials and Building Structures, Delft, Netherlands.

[**]   Research Engineer at the Department of Steel Structures, Institute TNO for Building Materials and Building Structures, Delft, Netherlands.

[***]   European Convention for Steel and Coal

1. INTRODUCTION

To solve the capacity and handling problems in storage buildings, racks are often used. As a consequence of the constructional requirements, storage racks are mostly fabricated of cold-formed sections (see [1]). Several rack types are used, e.g.: pallet racks (braced and unbraced, Fig. 1), drive-in and drive-through racks (Fig. 2) and cantilever racks. All these rack types possess constructional properties to which no attention has been paid in national or international steel building codes, especially as regards unbraced racks (see 2.). This lack was filled by the individual rack manufacturers in that they had to design a rack; generally acceptable and uniform rack design was then not possible.

Fortunately, several (draft) national recommendations have meanwhile been presented in Europe (e.g. [2] - [6]). However, there is still no pertinent uniformity in Europe, and that causes trade barriers. Furthermore some points in rack design are not solved yet.

Therefore a European research program was started within the FEM[x], after a Dutch initiative. The program is financially supported by the European steel industry and the ECSC. The aim of this research program is to draft European recommendations for steel pallet, drive-in and drive-through racks. These recommendations are planned to be completed by late 1978.

To avoid unnecessary duplication of research activities, and to come to harmonisation of design rules in Europe and the U.S., arrangements have been made between RMI[xx] and FEM to exchange information.

----

x)   Fédération Européenne de la Manutention

xx)   Rack Manufacturers Institute

2. CONSTRUCTIONAL RACK PROPERTIES

As a consequence of its constructional design, a storage rack differs very much from a traditional steel framework by the following properties:

- Perforated, thin-walled uprights (Figures 3 and 4).

- Connection type (Figures 3 and 4).

  For practical reasons, readily adjustable beams and cantilever brackets are wanted in pallet racks and drive-in or drive-through racks, respectively. For this purpose, most beams are provided with connectors which can be hooked into the perforations of the uprights.

- Type of "foundation" (Figure 5)

  The uprights are provided with relatively thin base plates, not always bolted or anchored to the floor.

- Influence of the pallets on the constructional behaviour of a rack structure.

  Most pallets have also a constructional function, as:

  . lateral bracing element for the beams, because of bending stiffness and diaphragm action;

  . shear element (diaphragm action) in a braced pallet rack to couple the unbraced front frame with the braced rear frame;

  . shear element (diaphragm action) to distribute the horizontal load over several upright frames.

3. ORGANIZATION OF THE RESEARCH PROGRAM

The ECSC research program on steel pallet, drive-in and drive-through racks contains the following subjects (Fig. 6):

- System sections (Belgium, France)

  Establishing the effect of perforations on the static values of a perforated member.

- Beam-upright connections (Netherlands).

  Determination of the rotation stiffness of the beam-upright connections as a function of several parameters. Establishing a standard testing procedure.

- Computer program (Belgium).

  Drafting of a computer program to calculate unbraced pallet racks, including non-lineair behaviour of the beam-upright connections.

- Stability of unbraced pallet racks (Netherlands).

  Deviation of abacuses to get a quick insight in the ultimate load of a rack with regard to frame instability. Influence of the end condition of the upright at the floor.

- Stability of beams (Netherlands).

  Determination of the influence of the pallets on the maximum load at the instant of lateral buckling for different beam sections.

— European recommendations (Netherlands, Belgium, France).

The final aim of this research program is to draft European recommendations. A drafting committee has been formed; its members are from the laboratories involved and representatives from the industry.

Besides the above mentioned research on racking, a preliminary investigation is carried out on steel shelves. This part of the program is carried out in the U.K., at Strathclyde University.

UNBRACED PALLET RACKS

One of the most important problems is to develop a justifiable calculation method to determine the ultimate load with regard to frame instability of unbraced pallet racks (Fig. 7). By justifiable is here meant:

(a) The applied calculation model has to result in a lower limit of the carrying capacity.

(b) This lower limit should not be too conservative. Rack design is to be optimal because of mass production.

(c) Some of the basic properties of the components cannot be calculated; they have to be determined by correct standard test procedures.

The ultimate vertical load with regard to frame intability is a function of the following parameters:

(1) Rotation stiffness of the beam–upright connection, c_b.

(2) Rotation stiffness of the floor-upright connection, c_f.

(3) Bending stiffness of the upright; moment of inertia I_u, beam distance h.

(4) Bending stiffness of the beam; moment of inertia I_b, beam length ℓ.

(5) Initial out of plumbness (unloaded condition).

(6) External horizontal loads.

Several of the above parameters form part of the ECSC research. In this publication, attention will be paid to the problem of frame instability and the parameters determining it , as for as the Dutch part of the ECSC research is concerned.

5. ROTATION STIFFNESS OF BEAM-UPRIGHT CONNECTIONS

5.1 Test program

As has been stated above, most pallet rack beams are provided with connectors which can be hooked into the perforations of the uprights (Figures 3 and 4). These hooked connections have the following characteristics:

(a) A relatively small rotation stiffness with regard to connections customary in steel buildings;

(b) A certain looseness, caused by the always existent play necessary for simple adjustment;

(c) An aberrant constructional design of the hooked connections used by rack manufacturers, so there will be a mutually different behaviour.

These characteristics make the hooked connection unsuitable for general calculation rules, existing at the moment for example for bolted, welded or riveted connections in building structures. This results in the necessity of determining the behaviour

of hooked connections by tests.

The behaviour of the hooked connections used in racks can be well described by means of a moment-rotation diagram (M-ϕ diagram), because of their constructional function.

The following properties of the hooked connection are important with regard to rack design (Fig. 8):

(1) M_u = ultimate moment

(2) c_b = rotation stiffness (b: beam and bracket)

$$c_b = \frac{d\,\{f(\phi)\}}{d\phi}$$

(3) ϕ_ℓ = angle of looseness

= rotation at M is zero or almost zero

(4) $\phi_{\ell h}$ = ϕ_ℓ in case of + M, and an initial horizontal position of the beam part.

(5) $\phi_{\ell m}$ = maximum value of ϕ_ℓ

In general c_b varies with the rotation ϕ , as is shown in Fig. 8. However, at the moment constant c_b-values are used in case of hand calculations, (e.g. [7]), but also in case of computer calculations[*] (calculation of the partially fixed pallet rack beams or of frame isntability). Therefore, some constant c_b-values are investigated. The form of the M-ϕ diagram makes that several definitions of a constant c_b-value are possible (Fig. 8).

----

[*] It was also planned to develop, as a part of this ECSC research on racks, a computer program which would be able to handle a non-lineair M-ϕ diagram. Unfortunately this computer program will not be available within a short time.

The research on hooked connections was mainly intended to:

(i)   draft a standard testing procedure for hooked connections;

(ii)   give uniform rules for the interpretation of the M-ϕ diagram to
        get design values for M_u, c_b and ϕ_ℓ.

To attain this object, the influence of five parameters had to be investigated:

a. Connection type

   Two types are investigated with the most important difference that type 1

   (Fig. 3) did not possess any play between the upright-flange and the connector

   (Fig. 9), contrary to type 2 (Fig. 4) with a play of about 4 mm.

b. Test set-up

   Two different test set-ups were investigated:

   - Cantilever set-up according to [2] and [8] (Fig. 10)

   - Cross set-up (Fig. 11)

c. Lever arm

   In both test set-ups, the lever arm 'a' is equal to the moment-shear force

   ratio $\frac{M}{S}$. In case of a conical perforation form (types 1 and 2), the connector

   will be pinched to the upright-flange by shear force S. Because of this action,

   the connection becomes stiffer. A high $\frac{M}{S}$ - ratio ('a'-value) means a relatively

   small S-value and thus a smaller connection stiffness. Some practical 'a'-values

   are given in Table 1.

   Most hooked connections applied have a rotation stiffness of about 15×10^3 à

   100×10^3 Nm/rad .

Based on this, and on the above calculated 'a'-values, the following two lever

arms have been used in the test series to investigate their influence.

- a relatively short arm: 'a' = ca. 125 mm

- a relatively long arm: 'a' = ca. 500 mm

d. Preloading_the_connection

As appears from Fig. 8, a beam-upright connection might act as a hinge at low

beam loads, because of looseness. This means $\frac{M}{S}$ = 0. With the test set-ups

applied, the influence of the shear force on this first part of the M-ϕ diagram

cannot be determined (tests: $\frac{M}{S}$ = constant $\neq$ 0). Therefore, some tests have

been carried out with preloading the connection by S only: S_{pre} = 1000 N

'a' = about 500 mm

(a large lever arm results in a relatively important influence of S_{pre}).

e. Looseness_(slip)_of_the_connection

To investigate the possibility of determining the angle of loosenss, $\phi_{\ell d}$, to

be used in design calculations, separately form the cantilever or cross test set-ups,

some tests have been carried out according to the standard looseness test procedure,

prescribed in [2] (Fig. 12),

N.B. The influence of the beam height on M_u and c_b has moreover been investigated.

5.2 Test set-up

As stated above, the connection tests have been carried out with 2 test set-ups, the cantilever and the cross set-up.

Attention has been paid to the following points:

(a) The lateral displacement of the beam end has been prevented (Fig. 10). This is necessary to simulate the real behaviour:

   - pallet rack: beam between two uprights
   - drive-in and drive-through rack: cantilever brackets are connected by beams (Fig. 13).

(b) The beam part has been horizontally positioned with regard to the vertical upright part. The beam possesses a similar position as in a pallet rack, which is important because of the magnitude of $\phi_{\ell h}$. The position of the origin O in Fig. 8 is depending on the initial slope between beam and upright.

(c) The measuring of local deformations of the beam part has to be prevented.

(d) The lever arm has been measured from the point of load application to the point where the shear force is transferred. The latter point is where the hooks catch the upright.

(e) Load application by means of a long pin ended strut (Fig. 10). In this way, a minimum of secondary normal forces are generated because the application point is able to displace laterally in the plane of the beam part. These displacements are a result of beam rotation.

5.3 Test results

Test results and conclusions are described in [9] .

Besides ultimate moment M_{ul} and angle of looseness $\phi_{\ell h}$, the c_b-values according to the following definitions (Fig. 8) were determined from the measured M-ϕ curves:

- c_{b1} , when unloading the connection;

- c_{b2} , when loading up to 0.5 M_{ul};

- c_{b3} , when loading up to 0.67 M_{ul};

- c_{b4} , mean c_b-value when loading up to 0.67 M_{ul}, including $\phi \leq \phi_{\ell h}$: $c_b = 0$.

5.3.1 General remarks

The c_{b1} definition is a meaningful one, as at one beam side the connection is unloaded because of the lateral displacement of an unbraced pallet rack. From available computer results it even appears that in most cases the moment reverses its sign, shorly before frame instability occurs.

This means that at the unloaded connection the maximum angle of looseness will at a certain moment be passed, and not only $\phi_{\ell h}$ (Fig. 8).

Additional tests to investigate this problem will be carried out in the near future.

The test results showed some considerable scatter, which hampers a statistical interpretation because of the relatively few tests, especially for the type 1 connection (Figures 14 - 18). This scatter is probably caused by important form deviations of the investigated beam-upright connections with respect to each other. The measured c_{b4}-values, including the influence of

$\phi_{\ell h}$, showed the largest scatter (type 1: maximal +78% and -57% with respect to the mean value; type 2: maximal +18% and -16% with respect to the mean value).

Because the connection properties, including the angle of looseness $\phi_{\ell h}$, are very important with regard to the carrying capacity of unbraced pallet racks, design values for c_b and ϕ_ℓ have to be determined carefully. This means:

(a) Besides $\phi_{\ell h}$, it is also important to know the maximum value $\phi_{\ell m}$ (Fig. 8) to determine a design value of ϕ_ℓ, because the position of the origin O in the ϕ_ℓ -traject very much depends on the position of the connector with regard to the upright flange and perforation side (Fig. 19). As mentioned above this position can show some considerable scatter, with the possibility that in one rack beam-upright connections are present with the most unfavourable position of the connector.

(b) One has to choose tes pieces from different parcels of finished products, because the position of the connector depends on the fabrication process. This can change from time to time, and from mechanic to mechanic. If the connector is automatically welded to the beam, the position of the connector will of course be more constant.

5.3.2 Ultimate moment

Contrary to the measured c_b- and ϕ_ℓ-values, M_u was showing little scatter (less than 10% with regard to the mean value).

M_u showed a linear relationship with the beam height; at the instant of failure, the lever of the force at the hooks is equal to the beam height (Fig. 20).

5.3.3 Rotation stiffness

It appeared that the c_{b3}-values are most suitable in design because these values had the smallest scatter in most cases, whereas c_{b1} and c_{b4} showed an unaccaptable amount of scatter (Figures 14 - 17).

The c_{b1}-values in case of a decreasing moment on the connection were higher with respect to e.g. the c_{b3}-values in case of an increasing moment (Type 1: $\frac{c_{b1}}{c_{b3}} = 1.2$ to 2.7; Type 2: $\frac{c_{b1}}{c_{b3}} = 1.2$ to 1.8).

When loading a complete pallet rack to its maximum number of pallets, a part of the beam-upright connections will be unloaded (see also 5.3.1).

5.3.4 Lever arm

With the two connection types investigated, the M_u- and c_b-values show a certain decrease with increasing lever arm 'a'. In the case of c_{b3}, an increase of 'a' gives the smallest decrease of c_b. The decrease of c_b becomes more important at increasing beam heigt (Fig. 18).

5.3.5 Test set-up

The test results form the cross tests showed significantly higher values for M_u and c_b ($\frac{M_u\text{-cross}}{M_u\text{-cantilever}} = 1.$ to 1.2; $\frac{c_{b3}\text{-cross}}{c_{b3}\text{-cantilever}} = 1.$ to 1.5).

This was probably caused by friction problems at the supports with the cross tests, resulting in secondary normal forces in the beam part. To avoid secondary normal forces in the cantilever tests, the load was applied by a long pin-ended strut (Fig. 10).

5.3.6 Preloading

With the two investigated connection types, a preloading by $S_{pre} = 1000$ N did not show any increase of the measured c_b-values (Figures 14 - 18).

5.3.7 Looseness test according to Fig. 12

It was hardly possible to interpret the looseness test results because of
their considerable scatter.

5.4 Standard test procedure

As a standard test procedure for the beam-upright connections in pallet racks,
the cantilever test is recommended.

Test set-up (Fig. 10):

(a) See points a - e of 5.2.

(b) Length of the lever arm 'a' = 300 mm.

(c) No preloading.

Minimum number of tests: 6, because of the scatter involved.

Contrary to the tests carried out so far, it is also recommended to load the
connection during one test by M with a reversed sign compared with the
moment caused by the vertical pallet loads only (no sidesway). In this way,
the maximum angle of looseness, $\phi_{\ell m}$, can also be measured.

5.5 Standard interpretation

For 6 test results, the design values of M_u, c_{b3} and ϕ_ℓ have to be determined
from:

design value = mean value $\overline{+}$ 2 $*$ standard deviation

          - → minimum design value

          + → maximum design value

Depending on the rack detail, the following design values of the beam-
upright connection have to be taken into account:

(a) Beam design   : - maximum $\phi_{\ell h}$

                            - minimum c_{b3}

(b) Connection design : - minimum $\phi_{\ell h}$

                            - maximum c_{b3}

(c) Frame instability : - the largest value of: . mean $\phi_{\ell h}$

                                             . 0.5 * maximum $\phi_{\ell m}$

                            - mean c_{b3}

(With frame instability, mean values are allowed because of the large number of connections involved).

6. ROTATION STIFFNESS OF THE FLOOR-UPRIGHT CONNECTION

6.1 Function of the base plate

In the first place, base plates are used to spread the vertical load in order to prevent floor damage, and to ensure good transfer of forces. However, the base plate influences also the end condition of the heaviest loaded bottom portion of the uprights. This bottom portion will mainly govern the ultimate load with regard to frame instability, because the upright section is generally constant over its total length. Therefore, the floor-upright connection is very important with regard to the carrying capacity of an unbraced pallet rack. The floor-upright connection consists of a base plate with a thickness of about 3 - 8 mm, which protrudes about 15 - 25 mm with respect to the upright section, measured perpendicular to the plane of the upright-frame.

Sometimes - and with drive-in and drive-through racks, this should be good

practice - the base plates are provided with bolts or anchors (Fig. 5). However,

research was retricted to·base plates welded to the uprights and without bolts

or anchors.

Base plates without bolts or anchors may always be considered as a hinged end

condition. In case of a relatively stiff floor material (e.g. concrete), this is

a rather conservative assumption, as there may be a non-uniform stress distribution

under the base plate (Fig. 21). So a certain partial fixity may be expected.

5.2 <u>Test series</u>

The partial fixity of the uprgiht at the floor has been investigated with the

test set-up of Fig. 22. An electronic hydraulic servo-system was used to ensure

that the vertical load vector always passes through the centre of the base plate,

so M and V were exactly known at the base plate (no second-order influences; Fig. 23).

The following parameters will affect the degree of fixity:

(a) Floor condition

   Tests: flat concrete floor with quality B 22.5 (f'_{ck} = 22.5 N/mm^2), steel floor

(b) Base plate dimensions (Fig. 24).

   Tests: t   = 3, 5, 10, 40 mm

           b_1 = 80, 120 mm

           b_2 = 6, 10, 12, 15, 25 mm

           d_1 = 50, 60 mm

           d_2 = 10, 20 mm

(c) Upright dimensions b_1 and d_1

(d) The initial angle between the base plate and the floor, measured in and
perpendicular to the plane of the upright frame.

(e) $\frac{M}{V}$ -ratio; M = moment on the base plate

   V = concentrical compression force on the base plate.

Several combinations of $\frac{M}{V}$ have been regarded:

- $\frac{M}{V}$ = constant = $\frac{1}{2}b_1$ + e_1 (Fig. 24, with R is resulting force of M and V):

   . b_2 = 15; e_2 = 20; e_1 = -5 mm

   . b_2 = 15; e_2 = 5; e_1 = 10 mm

   . b_2 = 25; e_2 = 5; e_1 = 20 mm

   . b_2 = 25; e_2 = 15; e_1 = 10 mm

- V = constant = 20 kN, increasing M

- V = constant = 60 kN, increasing M

- $\frac{M}{V}$ -ratio according to Fig. 25. Fig. 25 has been calculated with (10) {page 27}
   and ℓ = 3.70 m; h = 2.00 m; I_b = 171 $\ast$ 10^4 mm^4; I_u = 80 $\ast$ 10^4 mm^4;

   c_b = 30 kNm/rad and c_f = 125 knM/rad.

   An increasing $\frac{M}{V}$ -ratio with increasing vertical load V corresponds better

   with reality. The value of c_f = 125 kNm/rad has been derived from the

   tests with $\frac{M}{V}$ = constant.

6.3 Test results

Test results and conclusions are described in [10] .

The moment rotation diagram (M-φ diagram) for the base plates has the same

form as that of the beam-upright connections: a non-linear course and a certain

angle of looseness (Fig. 8). The results with $\frac{M}{V}$ according to Fig. 25 are

summed up in Table 2, where:

- for t, b_1, b_2, d_1, d_2: see Fig. 24;

- $\overline{M}_u$ = mean value of the ultimate moment;

- $\overline{\phi}_\ell$ = mean value of the angle of looseness;

- $\overline{c}_f$ = mean value of the rotation stiffness of the floor-upright connection.

(mean value of three test results)

From Table 2, the following can be concluded:

(a) c_f increases about linearly with t, when t increases from 3 to 5 mm. The

   increase of t from 5 to 10 mm has no influence on c_f, which is in contradiction

   with Table 3. Table 3 gives the test results for $\frac{M}{V}$ = constant.

(b) M_u increases approximately with $b_1 \sqrt{t}$.

(c) ϕ_ℓ shows considerable scatter.

It appeared to be very difficult to derive from these results a general rule to

calculate c_f and M_u. A standard testing procedure will be very expensive. Moreover,

the test results showed considerable scatter for c_f (e.g. table 2, 't = 3mm, d_2 = 20 mm:

c_f = 140, 305, 310, 260 kNm/rad). This scatter is caused by the great influence

of form imperfections on c_f.

However, knowing a lower limit of the rotation stiffness of the end condition of the

uprights at the floor, will already be a good help towards designing pallet racks

as optimally as possible. Because of the design methods used at this moment, a constant

c_f = c_{f4}-value should be derived in accordance with the c_{b4}-value

for beam-upright connections. So c_{f4} is a mean rotation spring constant, which also covers the traject with $c_f = 0$ for $\phi \leq \phi_\ell$. (Only that part of the M-ϕ diagram has been regarded where $\phi \leq 20 \times 10^{-3}$ rad $= \frac{1}{50}$).

Taking into account that a pallet rack possesses several base plates (about 8 to 20) with different c_{f1}-values (low and high), it is suggested to use in frame instability calculations as a rather good lower limit (Fig. 26):

flat concrete floor: $c_f = c_{f4} = 50$ kNm/rad, if $t \geq 5$ mm

7. FULL-SCALE TESTS

7.1 Test program

The full-scale tests are included in the research program to compare the calculated ultimate loads by hand (see 8.), or computer calculations with real physical behaviour. Within these calculations, component test results on beam-upright and floor-upright connections have to be used. Then the relation between the component tests plus the applied calculation model can be checked against reality.

Five full-scale tests have been carried out with variation of the connection type and the end condition at the floor:

a. Bolted beam-upright connection ($c_{b4} = 30$ kNm/rad)

a1.: Ball supports ($c_f = 0$)

a2.: - Flat concrete floor with quality B 22.5 (f'_{ck} = 22.5 N/mm^2)

    - Base plate with (Fig. 24): t = 8 mm, b_1 = 80 mm, b_2 = 4 mm,

      d = 50 mm, d_2 = 6 mm respectively frame width.

b. Beam-upright connection with hooks (c_{b4} = 19 kNm/rad)

b1.: Ball supports (c_f = 0)

b2.: - Flat concrete floor with quality B 22.5 (f'_{ck} = 22.5 N/mm^2)

    - Base plate with (Fig. 24): t = 8 mm, b_1 = 80 mm, b_2 = 40 mm, d_1 = 50 mm,

      d_2 = 25 mm.

b_3.: An artificial base fixity of the upright with a spring constant c_f = 60 kNm/rad.

7.2 Test set-up

All the assemblies tested had three beam levels and two bays. The rack height
was about 4500 mm, so the beam distance was about 1500 mm. The beam length was 2800 mm.
The vertical load was partly applied by dead weight (about 10 kN per pair of
beams) and partly by horizontally movable hydraulic jacks. The loads applied
by the jacks were kept vertical by horizontal jacks. A horizontal load of 1%
of the vertical load was applied by dead weight via a cable and a pulley.
An overall view of test a2. is given in Fig. 27. In this case, an electronic
hydraulic servo-system kept the loads, applied by the vertical jacks, vertical
when sidesway of the rack occurred.

7.3 Test results

Evaluation of test results is currently in progress. However, the following
tentative conclusions can now be drawn:

(a) The racks collapsed because of frame instability.

(b) Influence of the floor:

    - Ball support compared with concrete floor:

$$\frac{V_{a2}}{V_{a1}} = 1.5 \; ; \qquad \frac{V_{b2}}{V_{b1}} = 1.4$$

    - Effective spring constant of the concrete floor:

$$\frac{V_{b2}}{V_{b3}} = 1.0$$

    N.B. A design value for c_f = 50 kNm/rad would here be a lower limit (V_{b3}: c_f = 60 kNm/rad).

    (V = total vertical force at failure).

(c) Test b_2: the fixing moment of the uprights at the floor, combined with the vertical loads, caused local failure of the uprights of the middle frame at the floor.

8. SIMPLE DESIGN FORMULA WITH REGARD TO FRAME INSTABILITY OF UNBRACED PALLET RACKS

8.1 Principle of calculation model applied

To derive a relatively simple hand design method to check frame instability, a calculation model is used to replace the stability problem by a stiffness problem ([11]); the latter is much easier to solve. The stiffness properties determine the compressive load at which instability occurs, e.g.:

Euler: $F_E = \dfrac{\pi^2 EI}{(K \ell)^2}$; Stiffness: E, I, K$\ell$

The relevant stiffness property with regard to frame instability is the frame-stiffness against lateral displacements. The calculation model is based upon this phenomenon.

The following basic assumptions are made (Fig. 28):

(a) The frame consists of individual, stable elements.

(b) The original frame with the load scheme (Fig. 28a) is assumed to be replaced by the same, unloaded frame, connected to a pin-ended strut on which the total load acts (Fig. 28b). This is permitted because if point a is fulfilled, the collapse load with regard to frame instability is independent of the way the load is spread over the frame. The pin-ended strut is connected to the frame in such a way that only a horizontal force can be transmitted. Both, the connection bar and the pin-ended strut, are infinitely stiff and weightless.

(c) The critical load, V_{cr}, with regard to frame instability is defined as the load at which, after release, the frame remains standing in the forced displaced position, and will not return to its original undeflected position.

This means that at load V_{cr} the moment equilibrium of the laterally displaced pin-ended strut is fulfilled (Fig. 28c):

$$V_{cr} = \frac{H_s}{u} h \text{ -- (1)}$$

In fact, the term $\frac{H_s}{u}$ represents the spring stiffness, c_{fr}, of the frame against lateral displacement (a force $H_s = c_{fr}$ gives the frame a displacement $u = 1$).

$$V_{cr} = c_{fr}h \text{ -- (2)}$$

The spring stiffness, c_{fr}, being known, critical load V_{cr} follows from relation (2).

- Stable equilibrium : $c_{fr} > \dfrac{V}{h}$

- Neutral equilibrium: $c_{fr} = \dfrac{V}{h} \rightarrow V_{cr}$

- Instability   : $c_{fr} > \dfrac{V}{h}$

Remark

A too large spring stiffness, c_f, is found, if the area of the area of moment diagram of the uprights from the original frame is larger than that of the infinitely stiff pin-ended strut, after a certain lateral displacement The maximum necessary reduction of c_{fr} belongs to the flexural buckling case of a bar fixed at the base and free at the top. A maximum difference then exists between the two areas of the area of moment diagram (Fig. 29):

Model:

$$\dfrac{H_s}{u} = \dfrac{3EI}{h^3} \rightarrow V_{cr} = \dfrac{3EI}{h^3}$$

Euler: Maximum recuction factor =

$$V_{cr} = \dfrac{\pi^2 EI}{(2h)^2} = \dfrac{\pi^2 EI}{4h^2}$$

$$= \dfrac{\pi^2}{4 * 3} = 0.82 \text{ ---------------------- (3)}$$

Thus far only a vertical load has been considered, but horizontal loads can also act on the frame simultaneously. Additionally a frame can have an initial out of plumbness, after erection and without load. Both influences mean that V_{cr} cannot be determined unequivocally any more (according to eq. (2)). From the moment equilibrium of the pin-ended strut, a relation is now obtained between the present vertical load, V, horizontal load H and initial out of plumbness S_o (Fig. 30):

$$Vu_t + Hh - H_s h = o \div V = \frac{(H_s - H)h}{u_t} \quad \text{--------------------------} \quad (4)$$

Where: $u_t = u + u_o$ = total lateral displacement

u_o = displacement related to S_o

If the stiffness of the frame c_{fr} $(= \frac{H_s}{u})$ is substituted into relation (4), this relation changes into:

$$V = \frac{c_{fr}h(u_t - u_o) - Hh}{u_t} \quad \text{--------------------------------------} \quad (5)$$

From relation (5) it appears that it is not possible to determine the permissible vertical load directly from V_{cr}, but has to be determined on the basis of stiffness or strength requirements. For example:

- At working state   : $S_w \le \frac{1}{200}$

- At ultimate limit state: $S_u \le \frac{1}{50}$

- Yield of the upright, yield of the beam or attaining M_u in the connector.

8.2 Calculation model applied to unbraced pallet racks

To determine the spring stiffness c_{fr} against lateral displacment of a pallet rack, the following assumptions have been made:

(a) The rack has a regular configuration. That is the same uprights, beams, beam distances and bay widths are applied.

(b) The rack has infinite length. This is a conservative assumption. A significantly higher critical load with regard to frame instability is found if the rack consists of three or fewer bays.

(c) Portion of the rack adjacent to the floor is determinign frame instability (Fig. 7). This assumption is valid when the rotation spring constant of the base plate-floor connection is relatively small, and/or when the compressive stress in the lowest part of the uprights is considerably larger than in the parts above. In many cases this condition will be satisfied.

On the basis of these three assumptions, rack portion ABCD (Fig. 7) is representative of the spring stiffness, c_{fr}, of the rack.

Points B and C at midspan of the beams can be regarded as hinges with free lateral displacements because of symmetry considerations. Point D has been chosen at the position of zero moment in that part of the upright. The position of D is therefore determined by:

- rotation stiffness at A (building floor);

- number of levels;

- bending stiffness of the upright with respect to that of the beam (rotation

stiffness of the beam-upright connection included);

- lateral deflections of the frame, which means that the position of D is
also a function of the present vertical load.

An appropriate position of D will be determined by computer calculations in combination with full-scale test results. Suppose D at $(1 + \alpha)h$ above the floor.

An expression similar to eg.(5) can be derived from Fig. 30.:

$$V = \frac{\{(u_t - u_o)\, c_{fr} - H\}\,(1 + \alpha)h}{u_t} \quad \text{------------------------- (6)}$$

If the dimensionless magnitude $S = \dfrac{u_t}{(1 + \alpha)h}$ is used (S = out of plumbness), eq. (6) becomes:

$$V_b = \frac{2c_{fr}\,(S - S_o)\,(1 + \alpha)h - H_b}{S} \quad \text{------------------------- (7)}$$

where, V_b and H_b are loads per bay.

The following design formulas can be derived ([7]) to calculate $\beta = \dfrac{1}{c_{fr}}$ to be used in eq. (7) and M_f (fixing moment at the floor):

a. <u>Hinges at the floor</u>

$$\beta = \tfrac{1}{2}h^2\,(1 + \alpha)^2\,(\tfrac{1}{c_b} + \tfrac{\ell}{6EI_b}) + \tfrac{h^3\,(1 + \alpha^3)}{3EI_u} \quad \text{--------------------------- (8)}$$

b. <u>Partially fixed at the floor</u>

$$\beta = \tfrac{1}{2}\gamma h \ell \ (1 + \alpha) \ (\frac{1}{c_b} + \frac{\ell}{6EI_b}) + \frac{h^3 \ (1 + \alpha^3)}{3EI_u}$$

$$- \frac{h^2 c_f}{4(EI_u + hc_f)} \ (\frac{\gamma \ell}{c_b} + \frac{\gamma \ell^2}{6EI_b} + \frac{h^2}{EI_u}) \qquad \text{------------------------------------ (9)}$$

$$M_f = \frac{c_f \ EI_u}{2\beta \ (EI_u + hc_f)} \ (\frac{\gamma \ell}{c_b} + \frac{\gamma \ell^2}{6EI_b} + \frac{h^2}{EI_u}) \ u \ \text{------------------------------------ (10)}$$

where,

$$\gamma = \frac{6hI_b c_b \ \{2(1 + \alpha) \ (EI_u + hc_f) - hc_f\}}{12\ell I_b c_b \ (EI_u + hc_f) + \ell c_f \ I_u \ (6EI_b + \ell c_b)} \qquad \text{------------------------------ (11)}$$

c. <u>Fully fixed at the floor</u>

$$\beta = \frac{\gamma h \ell}{4} \ (1 + 2\alpha) \ (\frac{1}{c_b} + \frac{\ell}{6EI_b}) + \frac{h^3}{12EI_u} \ (1 + 4\alpha^3) \ \text{-------------------------- (12)}$$

$$M_f = \frac{EI_u}{2h\beta} \ (\frac{\gamma \ell}{c_b} + \frac{\gamma \ell^2}{6EI_b} + \frac{h^2}{EI_b}) \ u \ \text{-- (13)}$$

where,

$$\gamma = \frac{6h^2 I_b c_b \ (1 + 2\alpha)}{(12 I_b c_b h + 6EI_b I_u + \ell I_u c_b)\ell} \qquad \text{--- (14)}$$

It is also possible to check the upright section directly below the first

beam level, if the out of plumbness S has been calculated from eq. (7) and

M_f from eq. (19) or eq. (13). On this section are acting:

- bending moment　　　:　$M \approx \frac{1}{2}(hH_b + ShV_b) - M_f$　---------------------------- (15)

- compressive force　:　$V = \frac{1}{2}V_b$　--- (16)

- shear force　　　　　:　$H = \frac{1}{2}H_b$　--- (17)

In the Figures 31 and 32, V_b - S curves are given; they were calculated from the

equations above (V_b = total vertical load on one bay):

Fig. 32:　h　$= 2.0$ m

ℓ　$= 3.7$ m

c_b　$= 30$ kNm/rad; c_f in kNm/rad

I_u　$= 0.80 * 10^6$ mm^4 ($\llcorner$80 - 50 - 5)

I_b　$= 1.71 * 10^6$ mm^4 (INP 100)

S_o　$= 0$

α　$= 0.5$

Fig. 33:　h, ℓ, I_u, I_b, α , same as in Fig. 31

$c_f = 125$ kNm/rad

$S_o = \dfrac{1}{750}$

$H_b = 0.01\ V_b$

NOTATION

The following symbols are used in this paper:

a   = lever arm

c_b = rotation spring constant of the beam-upright connection

c_f = rotation spring constant of the floor-upright connection

c_{fr} = spring stiffness of a frame against lateral displacement

E   = Young's modulus

h   = beam distance

H   = horizontal load

H_b = total horizontal load per bay

I_b = moment of inertia of a beam

I_u = moment of inertia of an upright

ℓ = beam length

M   = moment

M_f = fixing moment of the floor

M_u = ultimate moment

S   = shear force; out of plumbness

S_o = initial out of plumbness

S_{pre}= shear force with which the beam-upright connection was preloaded before any moment was acting

u   = lateral displacement

u_o = lateral displacement related to S_o

u_t = total lateral displacement= u_o + u

V   = vertical load

V_b = vertical load per bay

V_{cr} = critical vertical load with regard to frame instability

β = $1/c_{fr}$

ϕ = angle of rotation

ϕ_ℓ = angle of looseness

$\phi_{\ell h}$ = ϕ_ℓ in case of + M (Fig. 8) and an initial horizontal position of the beam part

$\phi_{\ell m}$ = maximum value of

LITERATURE
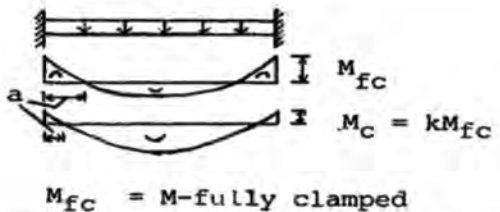
[1]   T. Peköz, G. Winter, "Cold-formed steel rack structures", Second Speciality Conference on Cold-Formed Steel Structures, Department of Civil Engineering, University of Missouri-Rolla, October 1973.

[2]   Storage Equipment Manufacturers Association - SEMA, "Interim code of practice for the design of static racking", April 1977, Great Britain.

[3]   Lager- und Betreibseinrichtungen Gütesicherung - RAL - RG 614, Juli 1977, Germany.

[4]   Syndicat des Industries de matériels de manutention - SIMMA, "Recommandations pour le calcul de rayonnages pour pallets", Juillet 1975, France.

[5]   SIMMA, "Recommandations pour le calcul des structures de stockage par accumulation", Octobre 1976, France.

[6]   Groep Stelling Fabrikanten - GSF, "Richtlijnen voor de berekening van stalen industriële magezijnstellingen - RSM 1977", Netherlands.

[7]   C.J. Tilburgs, R. Vis, "Simple design formula with regard to frame
        instability of unbraced pallet racks", TNO report BI-77-29/
        05.3.51256.

[8]   ANSI MH 16.1 - 1974, "Specification for the design, testing and
        utilization of industrial steel storage racks", U.S.

[9]   C.J. Tilburgs, F. Soetens, "Rotation stiffness of hooked connections in
        pallet, drive-in and drive-through racks", TNO report BI-77-27/05.3.51254.

[10]   C.J. Tilburgs, R. Vis, "Tests to investigate the degree of fixity of the base
        plates of uprights in pallet racks", TNO report BI-77-30/05.3.51254.

[11]   A. Bolten, "A simple understanding of elastic critical loads", The Structural
        Engineer, June 1976, No. 6, Volume 54.

Table 1: Practical 'a'-values

k	$\frac{a}{\ell}$	c_b [Nm/rad]		a [mm]	
		ℓ = 2400 mm	ℓ = 3700 mm	ℓ = 2400 mm	ℓ = 3700 mm
1	0.21	∞	∞	504	780
1/2	0.09	140×10^3	114×10^3	216	333
1/4	0.044	47×10^3	38×10^3	106	163
1/8	0.021	20×10^3	16×10^3	50	78

c_b calculated form k with:

- ℓ= 2400 mm: I_ℓ = 80 cm^4 (IPE 80)
- ℓ= 3700 mm: I_ℓ = 171 cm^4 (IPE 100)

M_{fc}

$M_c = kM_{fc}$

M_{fc} = M-fully clamped

Table 2: Base plate tests with $\frac{M}{V}$ according to Fig. 25

t	b_1	b_2	d_1	d_2	$\overline{M}_u$	$\overline{\phi}_\ell$	$\overline{c}_f$
mm	mm	mm	mm	mm	Nm	$\times 10^{-3}$ rad.	kNm/rad
3	80	10	50	15	700	0	90
	80	15	50	20	930	1	250
5	80	15	50	20	1000	9	450
	120	20	60	20	1750	2	330
10	80	15	50	20	1330	10	450

Table 3: Base plate tests with $\theta_1 = 10$ mm (Fig. 24)

t	b_2	d_2	floor material	ϕ_ℓ	c_f
mm	mm	mm		$x \cdot 10^{-3}$ rad.	knM/rad
5	12	20	concrete	5	125
	12	20	concrete	-5	100
	15	20	concrete	2	130
	11	20	steel	-6	100
10	15	20	concrete	11	225
	15	20	concrete	24	410
	15	20	concrete	19	230
	25	22	concrete	28	240
	15	20	steel	12	415
40	13	20	concrete	7	330
	12	20	steel	10	800
	13	20	steel	9	650
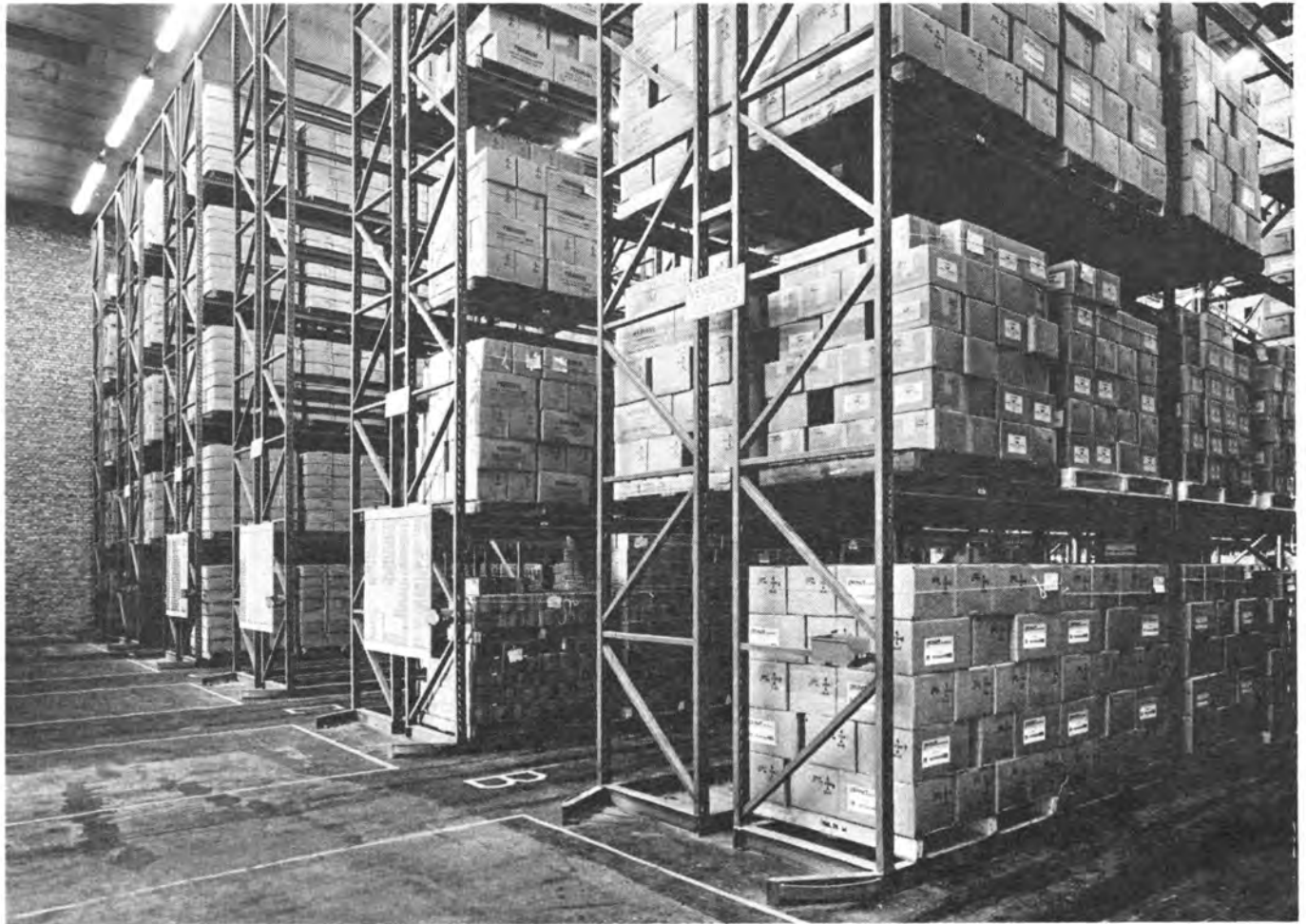
Fig.1 Example of a pallet rack

Fig. 2 Example of a drive-in and drive-through rack
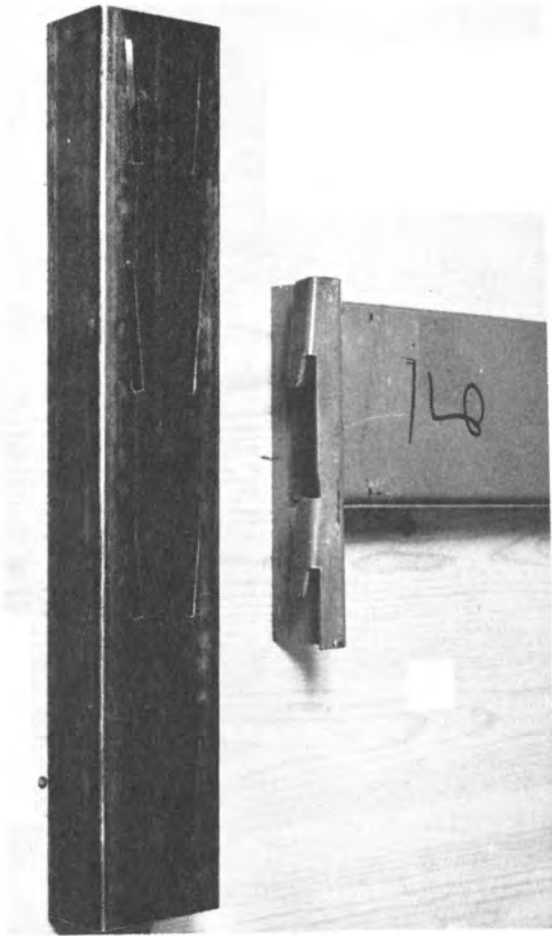
Fig. 3 Example of a beam-upright connection; connection type 1
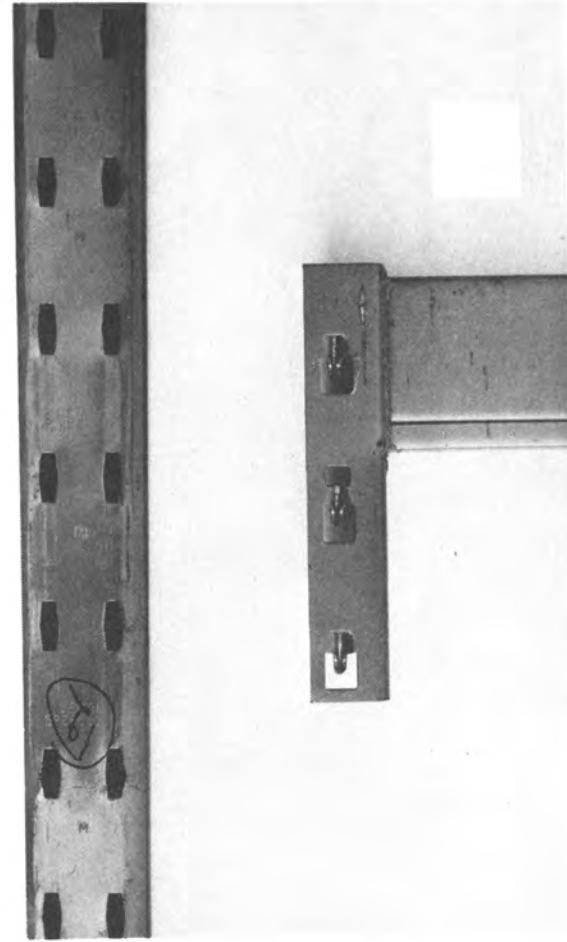
Fig.4 Example of a beam-upright connection; connection type 2
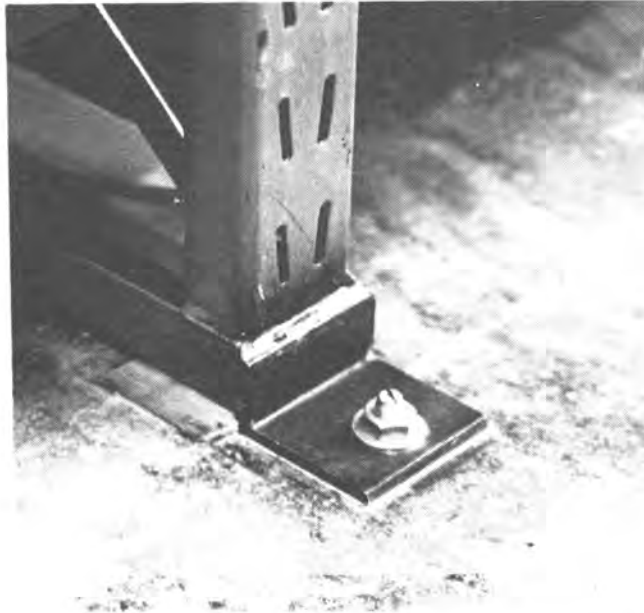
Fig. 5 Example of a base plate construction
(also without bolts or anchors)
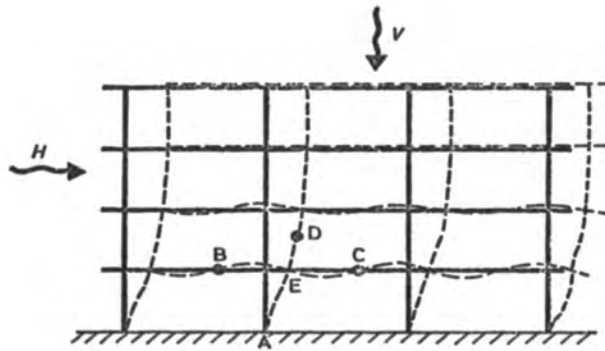
Fig. 7 Portion of the rack adjacent to the
building floor is determenative of
frame instability

EUROPEAN RESEARCH PROGRAM

Program		Executing country
Inventory and survey of literature		All participants
Influence of perforations on area, moment of inertia etc	calculation methods and/or standard tests	Belgium France
Beam upright connections	standard tests	Netherlands
Stability of unbraced pallet racks	computer progr.	Belgium
	hand calculation rules	Netherlands
	full scale tests	Netherlands
Stability of beams in pallet racks	influence of the pallets on the lateral buckling behaviour	Netherlands
Horizontal loads		Belgium Netherlands
European Recommendations		Belgium Netherlands France

Fig.6 Organisational scheme of the European research program on pallet, drive-in and drive-through racks
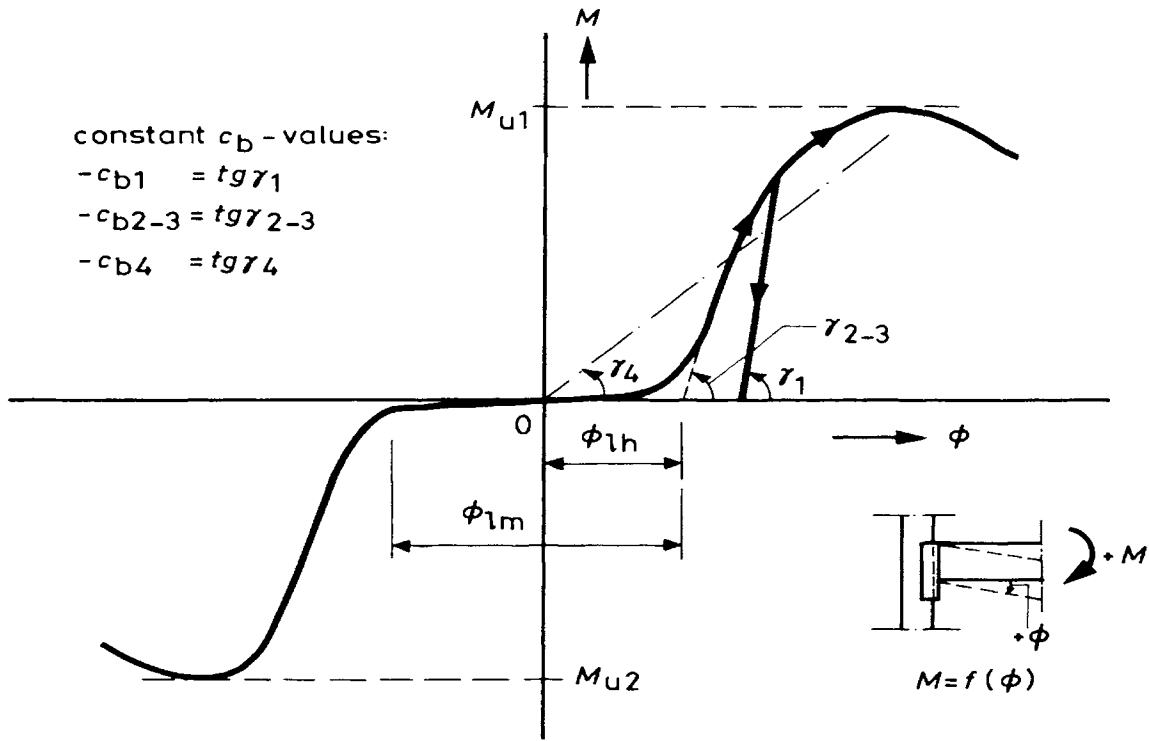
Fig.8 Qualitative rendering of a $M - \phi$ diagram of hooked connections used in racks
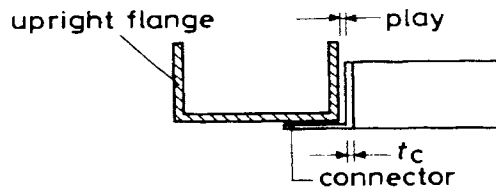
Fig.9 Position of the connector with regard to the upright flange
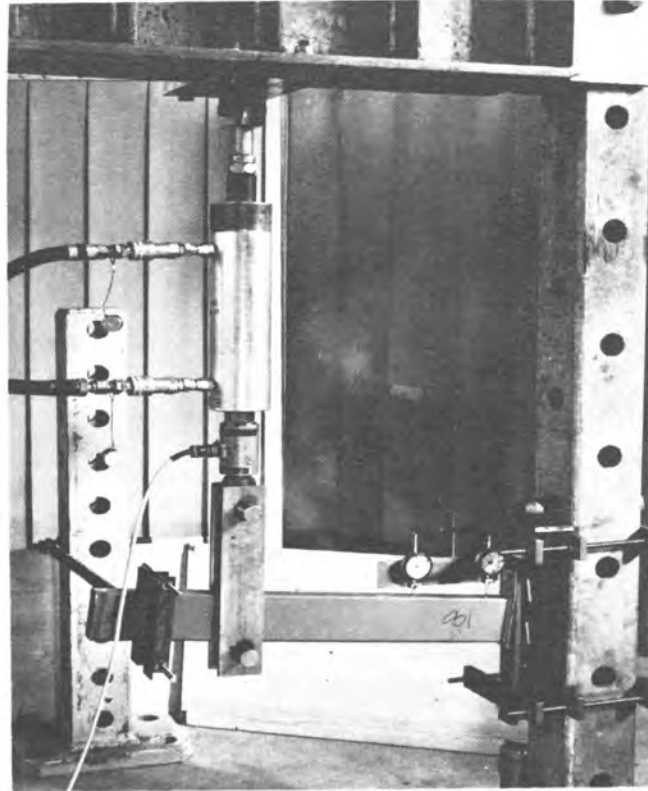
Fig.10 Cantilever test set-up; notice the way of
load application and the prevention of
lateral displacements of the beam end
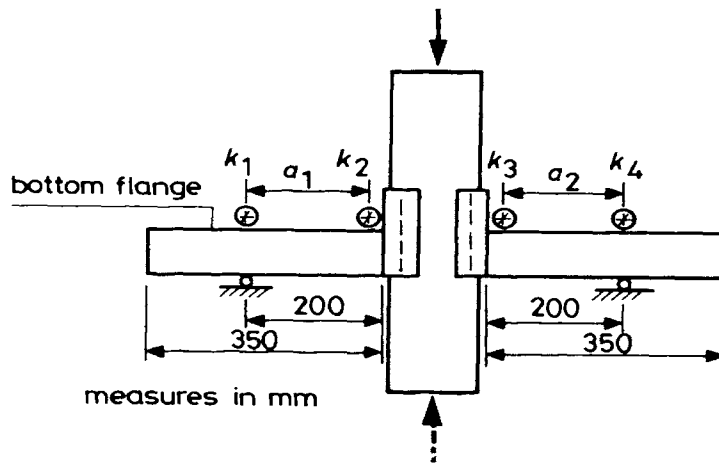
Fig.11   Cross set-up
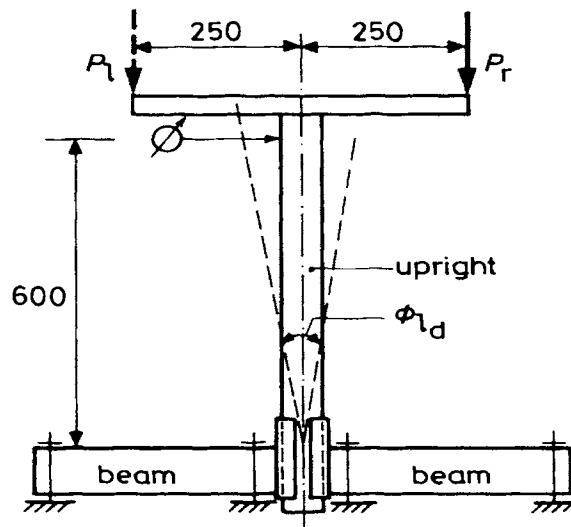
Test procedure

a. P_r = 500 N
b. P_r =   50 N
c. measurement r (mm)
d. P_l = 500 N
e. P_l =   50 N
f. measurement l (mm)
g. $\phi_{l_d} = \dfrac{|l - r|}{200}$

Fig.12   Looseness test in accordance with the
         SEMA code ([2])
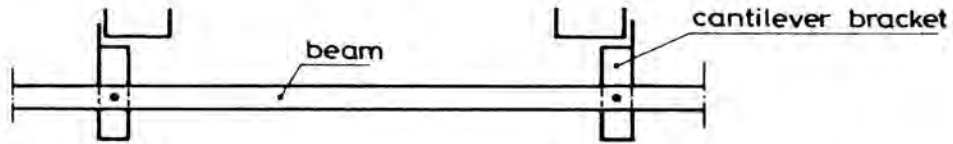
Fig.13 Lateral displacement of the brackets is impossible
      because of the beam and the opposite orientation
      of the brackets with regard to each other
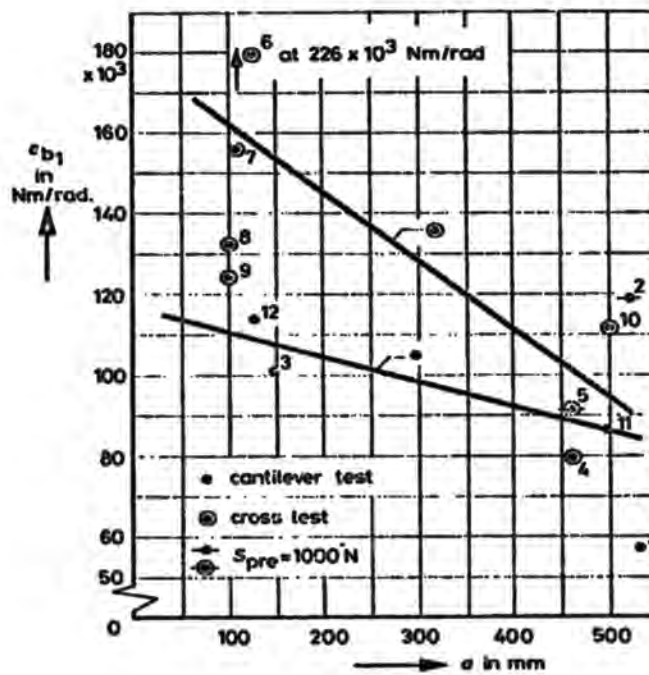
Fig.14 c_{b1}-values for type 1 connection with a
      beam height of 100 mm
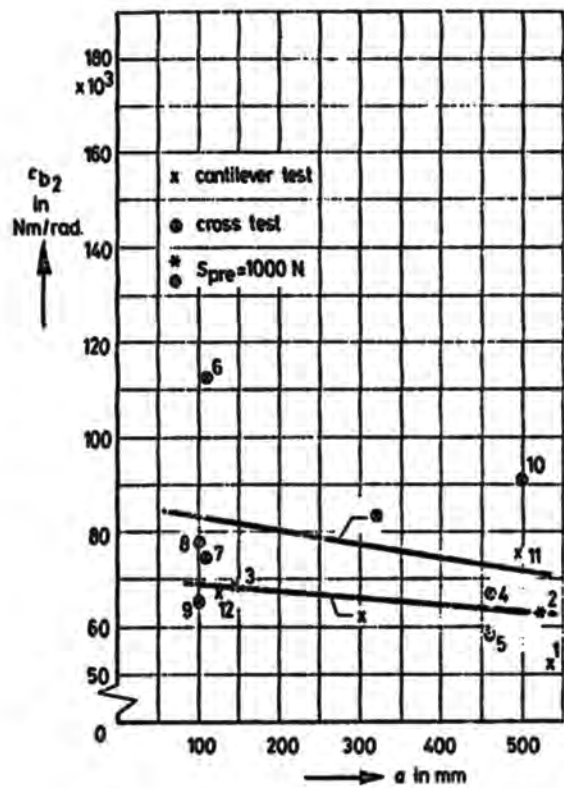
Fig.15 C_{b2}-values for type 1 connection with a beam height of 100 mm
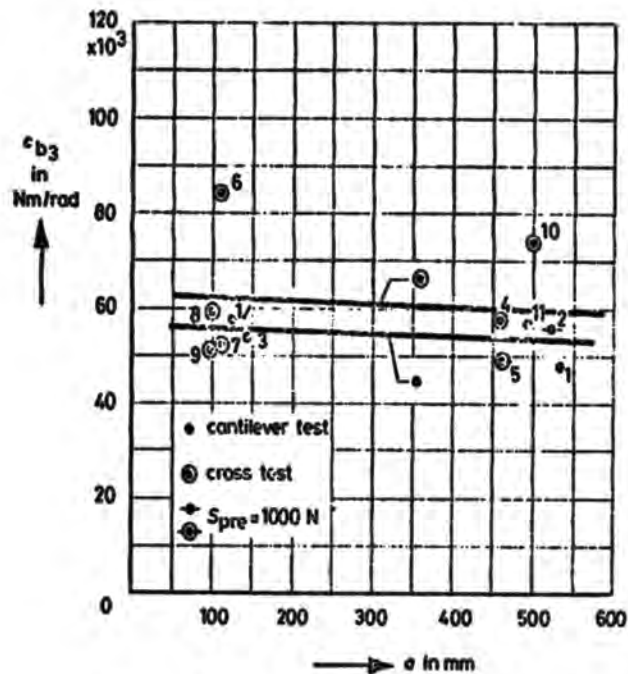
Fig.16 C_{b3}-values for type 1 connection with a beam height of 100 mm
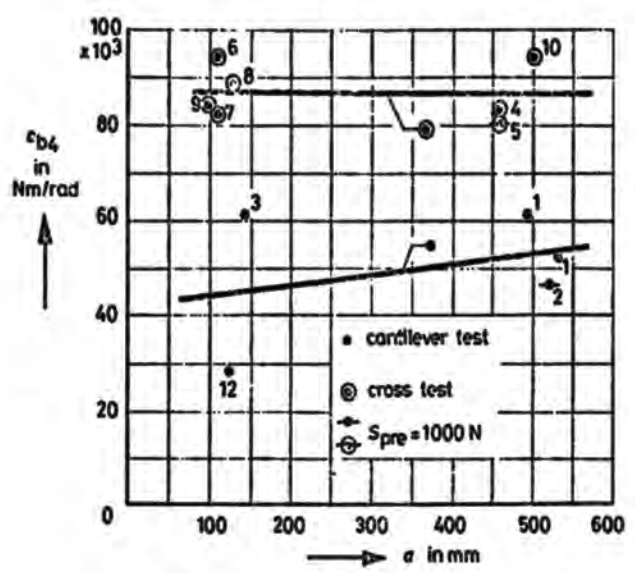
Fig.17 C_{b4}-values for type 1 connection with a beam height of 100 mm
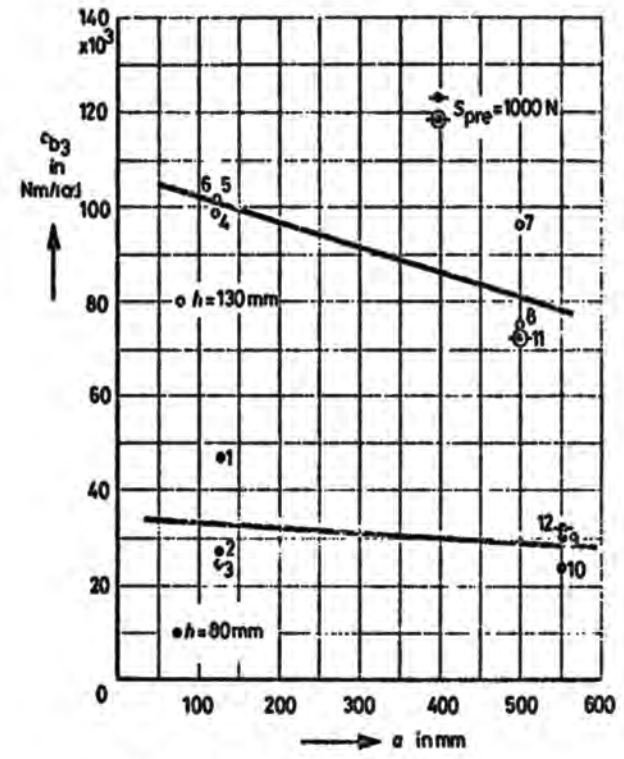
Fig.18 Results of cantilever tests on connection type 1 with beam heights of 80 mm and 130 mm
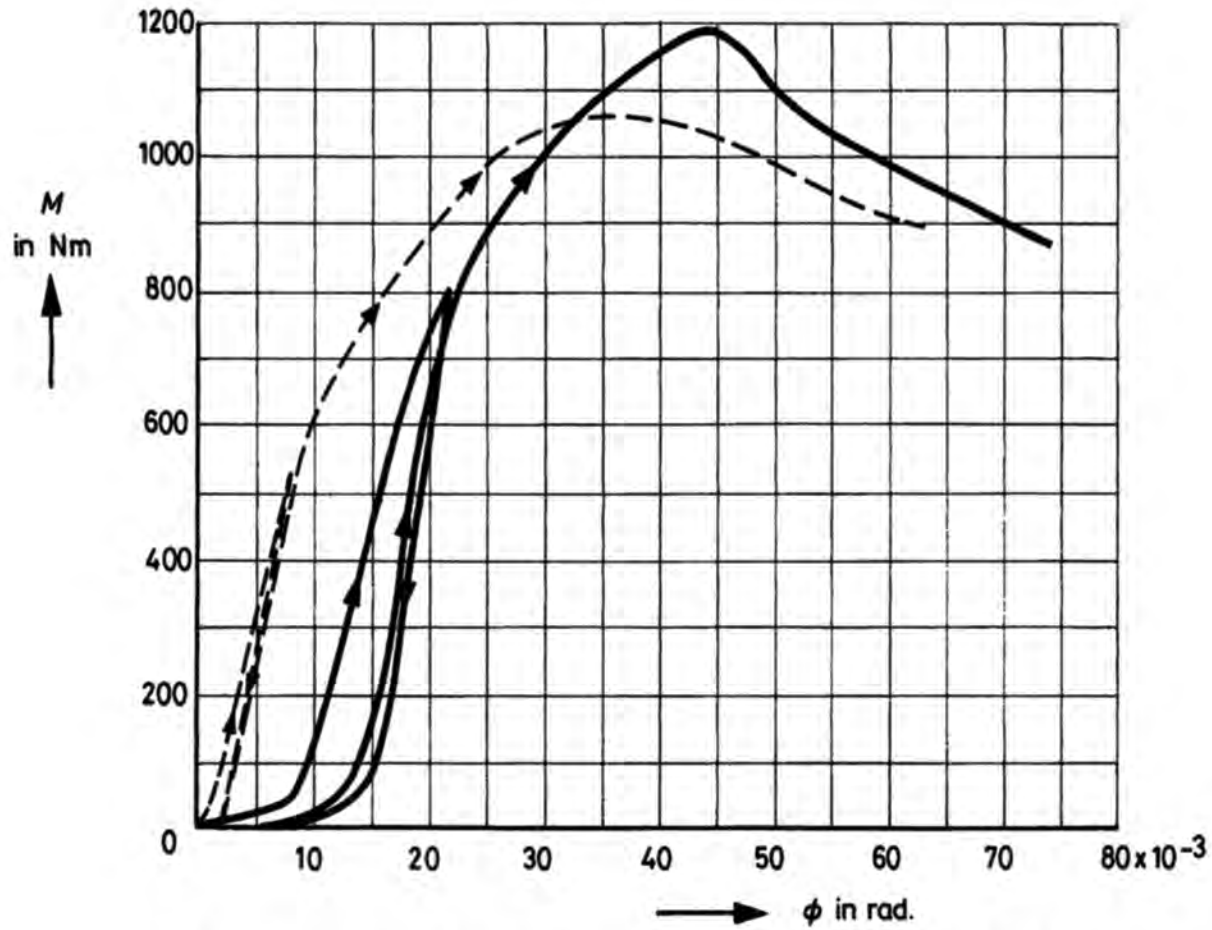
Fig.19   Results of two identical tests on connection type1 with a beam height of 100 mm ; notice the difference in the ϕ_{lh}-values

a=beam height of 130 mm

b=beam height of 80 mm
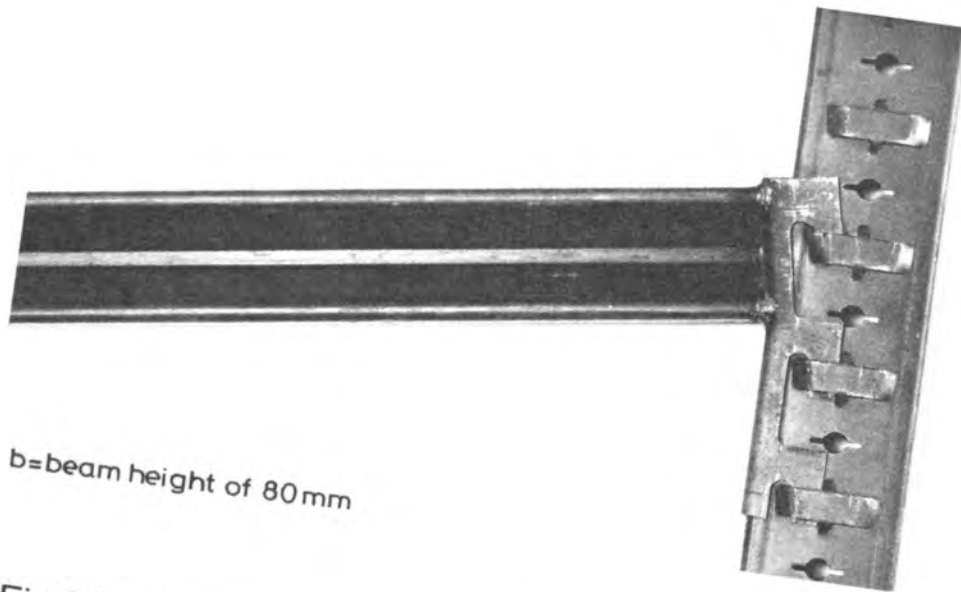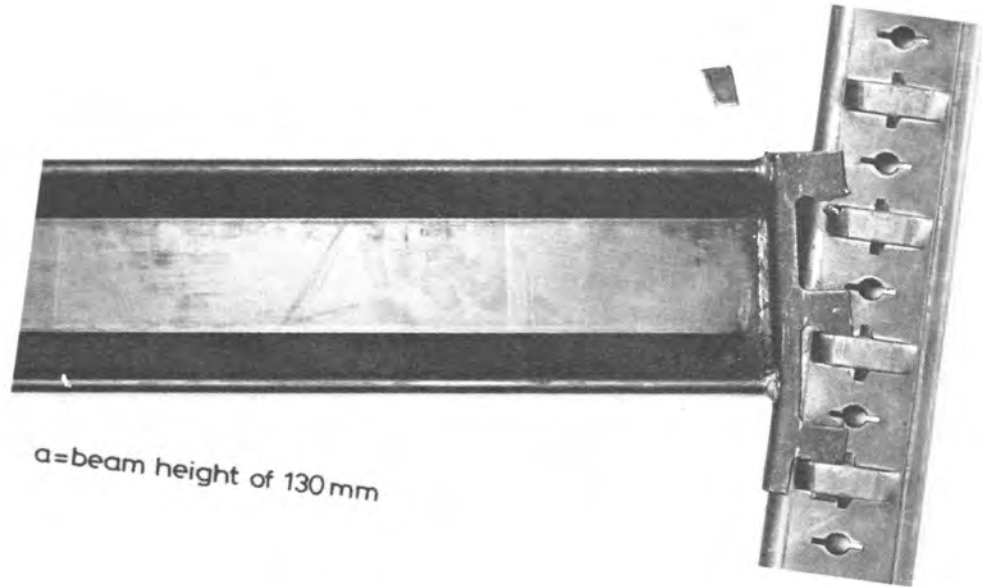
Fig.20 Failure modes of beam–upright connections with hookes
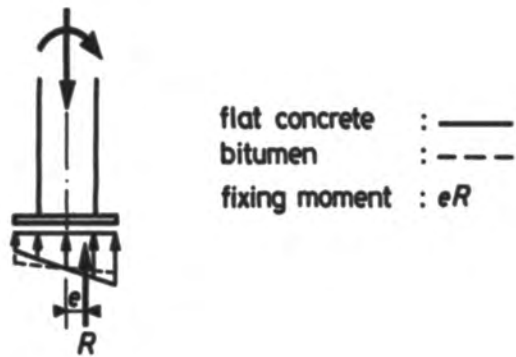
Fig. 21 Non-uniform stress distribution under a base plate

flat concrete : ⎯⎯⎯
bitumen : ⎯ ⎯ ⎯
fixing moment : eR
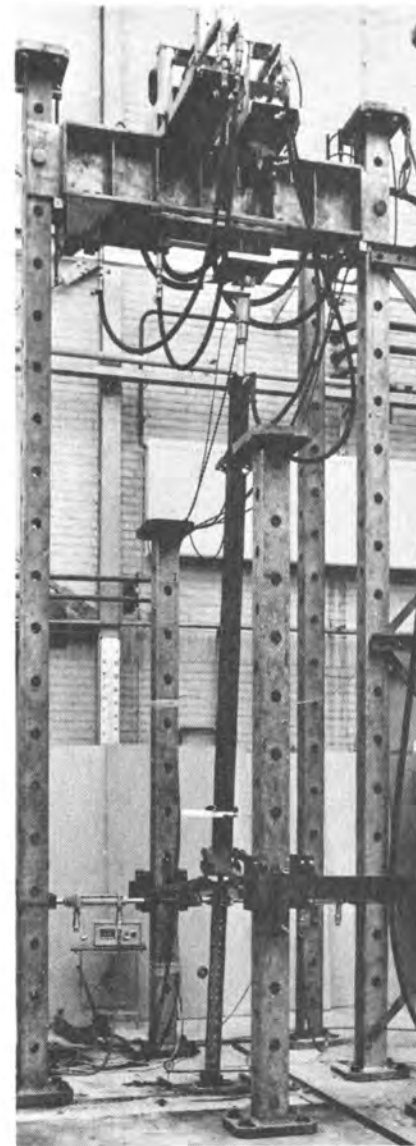
Fig. 22 View on a base plate test

actuator
loadcell
displacement transducer
s   signal of displacemement transducer
d   displacement
ball bearing
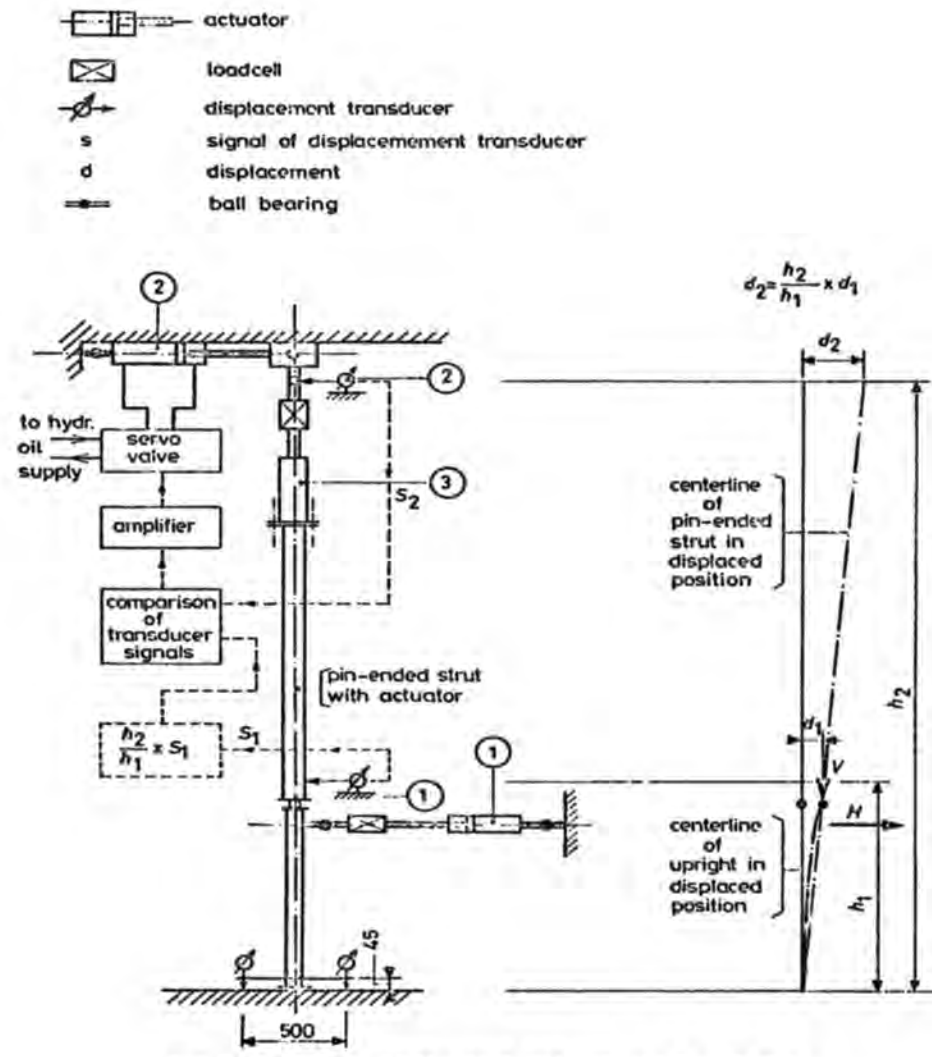
Fig. 23 Principle of the test set-up, used with the base plate tests
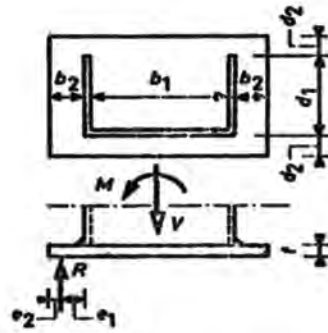
Fig. 24   Base plate dimensions
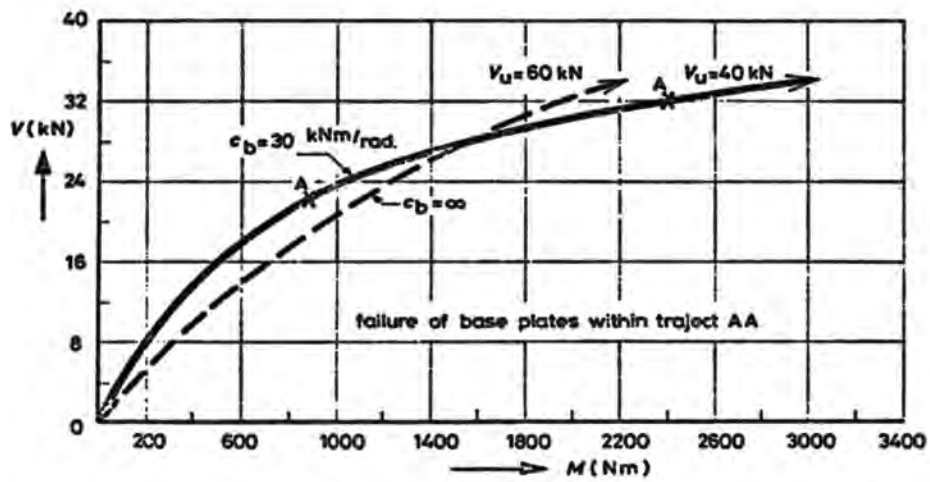
Fig. 25   M-V curve, used with tests summarized in table 2
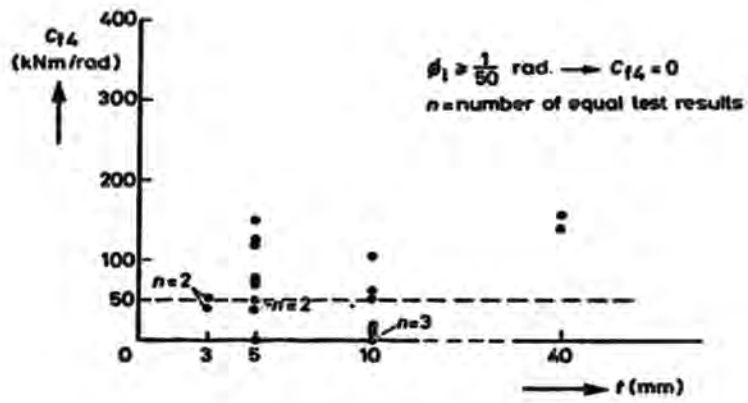
Fig.26   Test results of c_{f4}

a. frame

b. model

c. stability ∞ stiffness
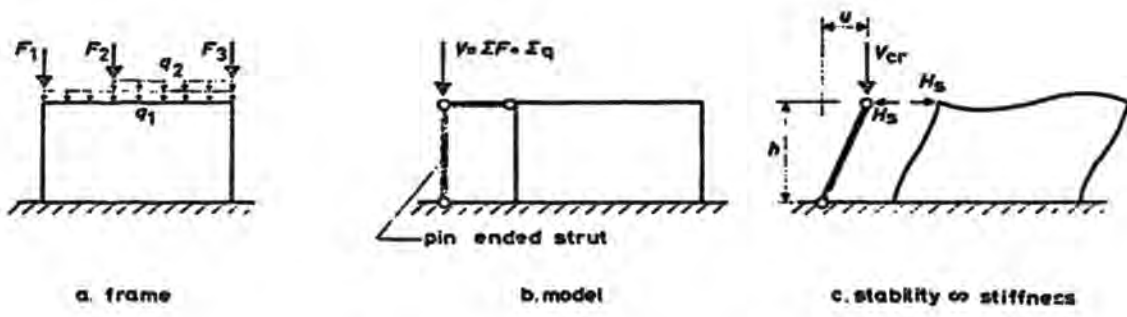
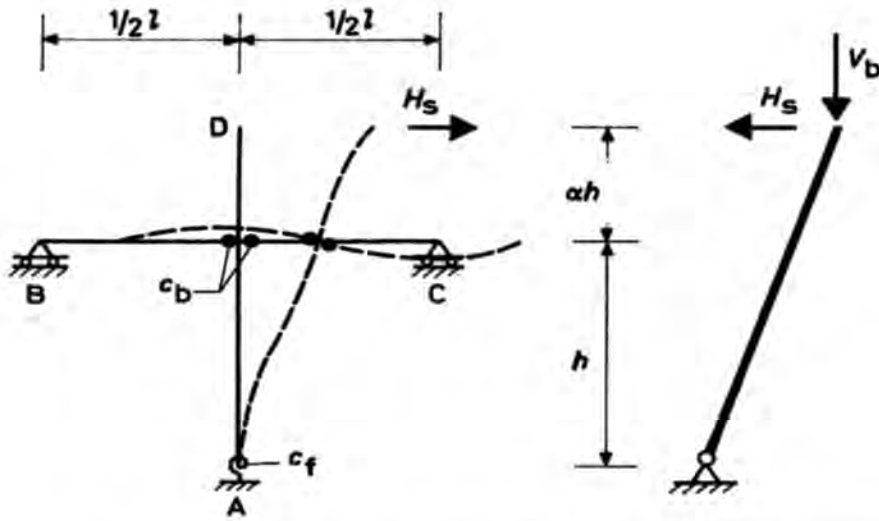Principle of the calculation model

Fig. 28
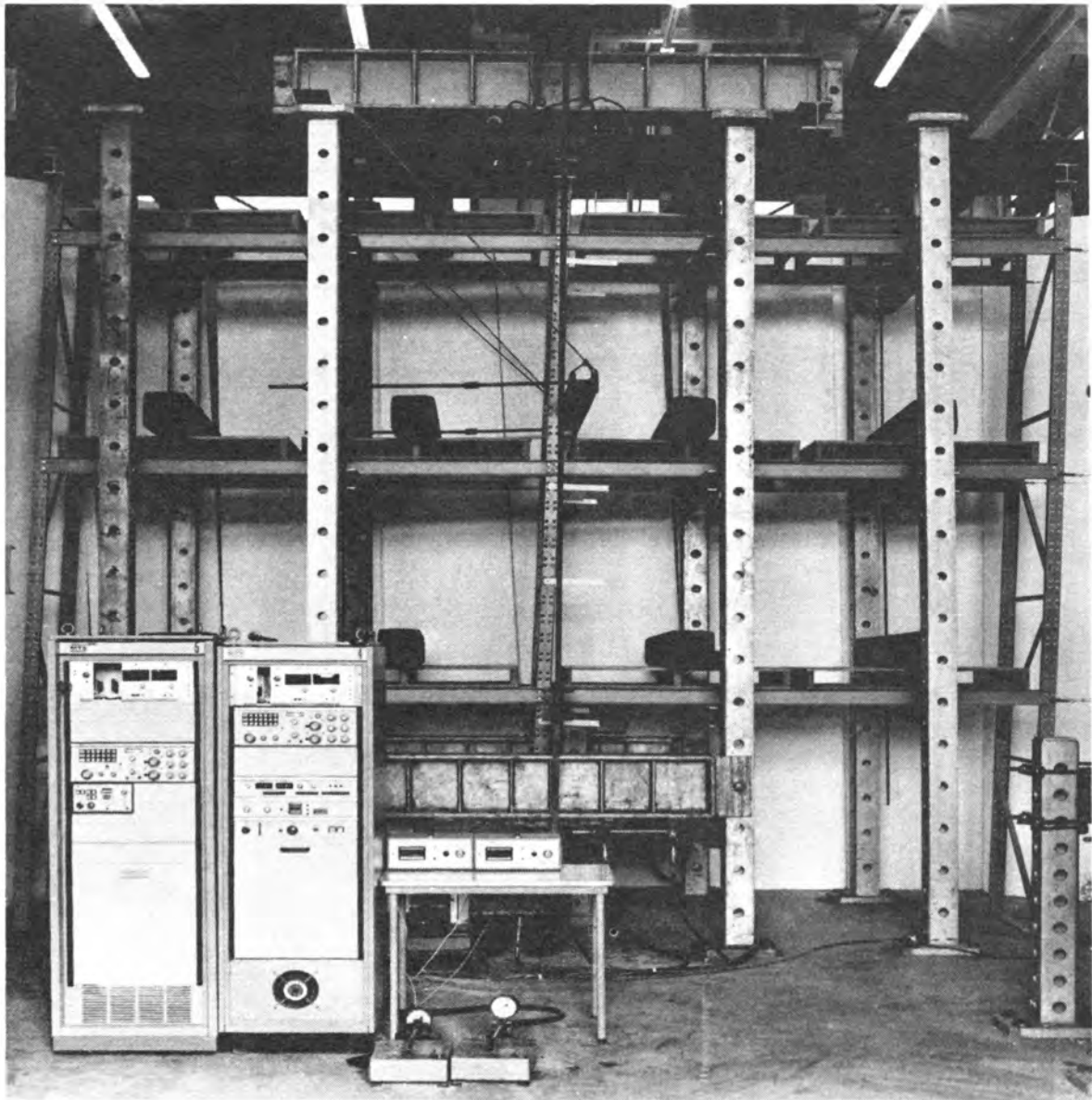
Fig.27 View on full-scale test no. a 2
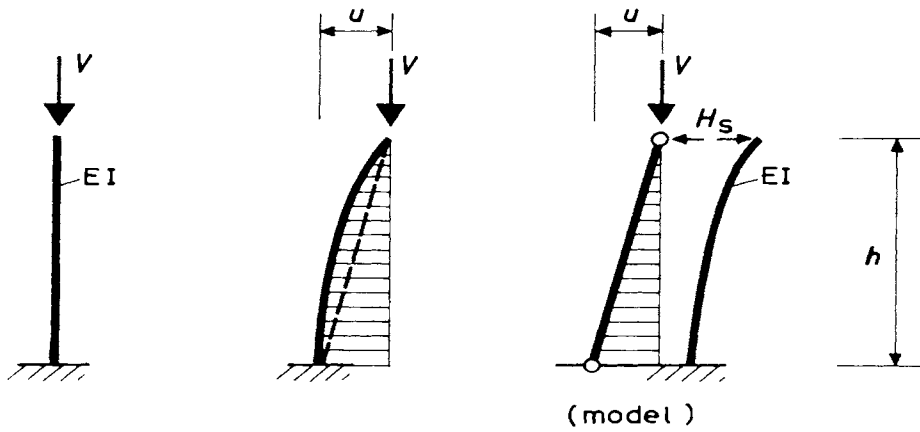
Model applied to a bar, fixed
at the base and free at the top.

Fig.29

u_o : no internal forces in the

rack $\rightarrow H_s = 0 \rightarrow c_f = \dfrac{H_s}{u}$
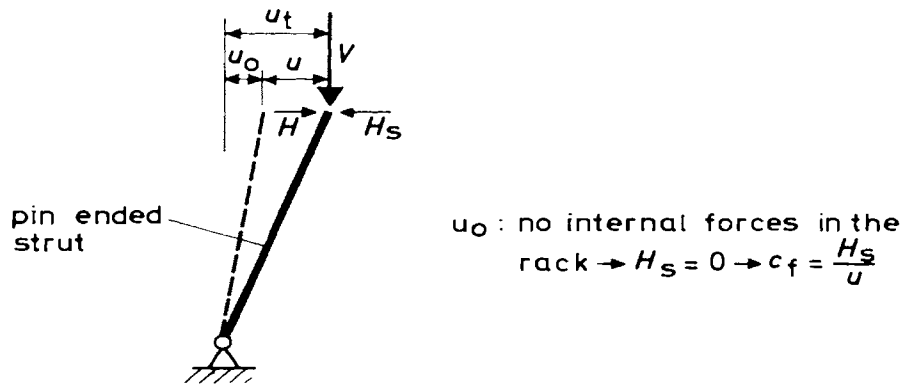
Forces at the pin-ended strut in case
of an initial out of plumbness u_0 and a
horizontal load H

Fig.30

c_b = Rotation spring constant beam upright connection.
c_f = Rotation spring constant floor upright connection.

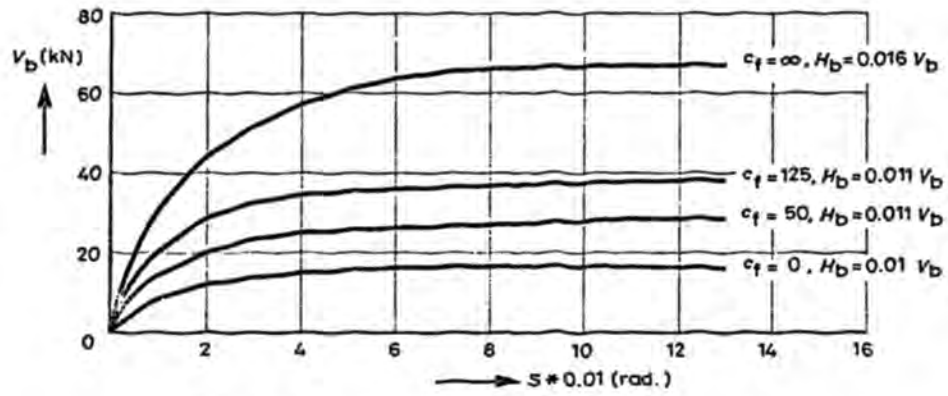Model with regard to unbraced
pallet racks.
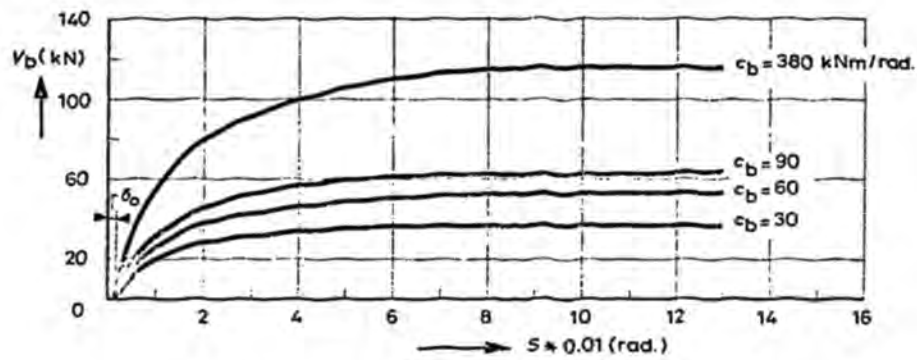
__Fig.31__

Fig. 32 $V_b - S$ curves with varying c_f-values

Fig. 33 $V_b - S$ curves with varying c_b-values